Wavelength Tunable Optical Second Harmonic Generation Suitable For Use With The LIGO Squeezer

Curtis Rau

November 27, 2015

Abstract

The purpose of this experiment was to construct an Optical Second Harmonic Generator (SHG) for advanced LIGO suitable for use with the Squeezer System. The performance of the advanced LIGO interferometers will be fundamentally limited by Shot Noise. One way of reducing shot noise in the output of the interferometer is to squeeze the vacuum state of the electromagnetic field the interferometer sees at its antisymmetric port. Second harmonic generation is necessary for the production of squeezed light. This paper touches upon the theory of squeezing, second harmonic generation, resonant optical cavities, higher-order modes in those cavities, and the Pound-Drever-Hall method. DISCLAIMER: This is only a draft. I have postponed the completion of this paper until after I have applied for graduate school. It has not been peer reviewed.

1 Second Harmonic Light in aLIGO

The interferometers implemented in advanced LIGO have a free spectral range that is much more stable than the frequency of the laser used to drive them (is this correct?). Thus they reject (via reflection) much of the classical noise the laser produces such as thermal and Josephson noise. The quantum noise contained in the output light from the interferometer, then, does not come from the laser, but rather stems from vacuum fluctuations which enter the antisymmetric port of the interferometer. The noise comes in two conjugate forms: radiation pressure and photon counting error. When the laser field and zero-point fluctuations are superimposed and impinge on one of the quasi-free-falling optics they perturb its position. This is the radiation pressure noise which scales with input power. When the signal leaves the interferometer it is recorded by a photodiode. Because photons are quantized, the act of measuring optical power is really an act of counting. This subjugates the interferometer signal to Poisson Counting Statistics where the relative standard deviation or specifically the uncertainty in the number of photons goes as $\sqrt{n}$. This source of error is known as *shot noise*, and it becomes increasingly problematic when output power is low. Originally shot noise was thought to arise from fluctuations in the input power, but Caves showed shot noise also is a product of vacuum fluctuations entering the antisymmetric port [3]. The zero-point fluctuations mix with the signal field produced at the beamsplitter giving rise to shot noise [1]. Shot noise is particularly relevant because the LIGO interferometers are operated on a dark fringe. Because one noise source dominates when optical power is high while the other dominates as it approaches zero, it stands to reason there would be some optimum amount of power such that the combined error from both sources (quadrature sum of these errors) is minimized. This occurs when the error in each conjugate noise source is equal, and the optimum power is given by equation 1.

$$P_{opt} \approx \frac{mc^2}{2\omega\tau^2 b^2} \tag{1}$$

[3, Eq. 1.2]. Optimal power for these interferometers is much higher than commercially available lasers are capable of producing, so

the accuracy of the LIGO interferometers
is fundamentally limited by shot noise.

What may be surprising is that the error due to shot noise can be reduced without increasing input power. Further the quantum nature of light actually allows shot noise to be below the Poison Counting Error, even though it is a counting measurement. Poison Counting Statistics only apply to *coherent states* such as the ground state

of a vacuum. The method for accomplishing this involves changing the state of the vacuum fluctuations the interferometer sees at its antisymmetric port.

Let me take a moment to present some of the major relevant ideas of quantum optics. In classical E and M we speak of electric and magnetic fields when describing a photon. Quantum optics prefers to work with two *field quadratures*. These are dimensionless quantities that oscillate in time with the associated classical analog.

$$X_1(t) = \sqrt{\frac{\epsilon_0 V}{4\hbar\omega}}\mathcal{E}_0 \sin(\omega t) \tag{2}$$

$$X_2(t) = \sqrt{\frac{V}{4\mu_0\hbar\omega}}B_0 \cos(\omega t) = \sqrt{\frac{\epsilon_0 V}{4\hbar\omega}}\mathcal{E}_0 \cos(\omega t) \tag{3}$$

[4, Eq. 7.27] Notice they have the same amplitude and are always out of phase by $\pi/2$. We can define the state of the field in Dirac Notation as $|\alpha\rangle$ where

$$\alpha \equiv X_1 + iX_2 \tag{4}$$

If we were to plot α in the complex plain it would always on the $X_1 = iX_2$ line because the two quadratures have the same amplitude. At this point the picture is a twist on a classical view, but in quantum mechanics we allow the two quadratures to take on any real value independent of one another (not sure if this is true). Which allows for much more exotic photon fields.

The uncertainty principle can be for the quadratures and for phase-number. Some uncertainty related equation are

$$\Delta\phi\Delta n = \Delta X_1 \Delta X_2 \geq \frac{1}{2} \tag{5}$$

$$\Delta n = \sqrt{\bar{n}} = |\alpha| \tag{6}$$

$$\Delta\phi = \frac{1}{2\sqrt{\bar{n}}} \tag{7}$$

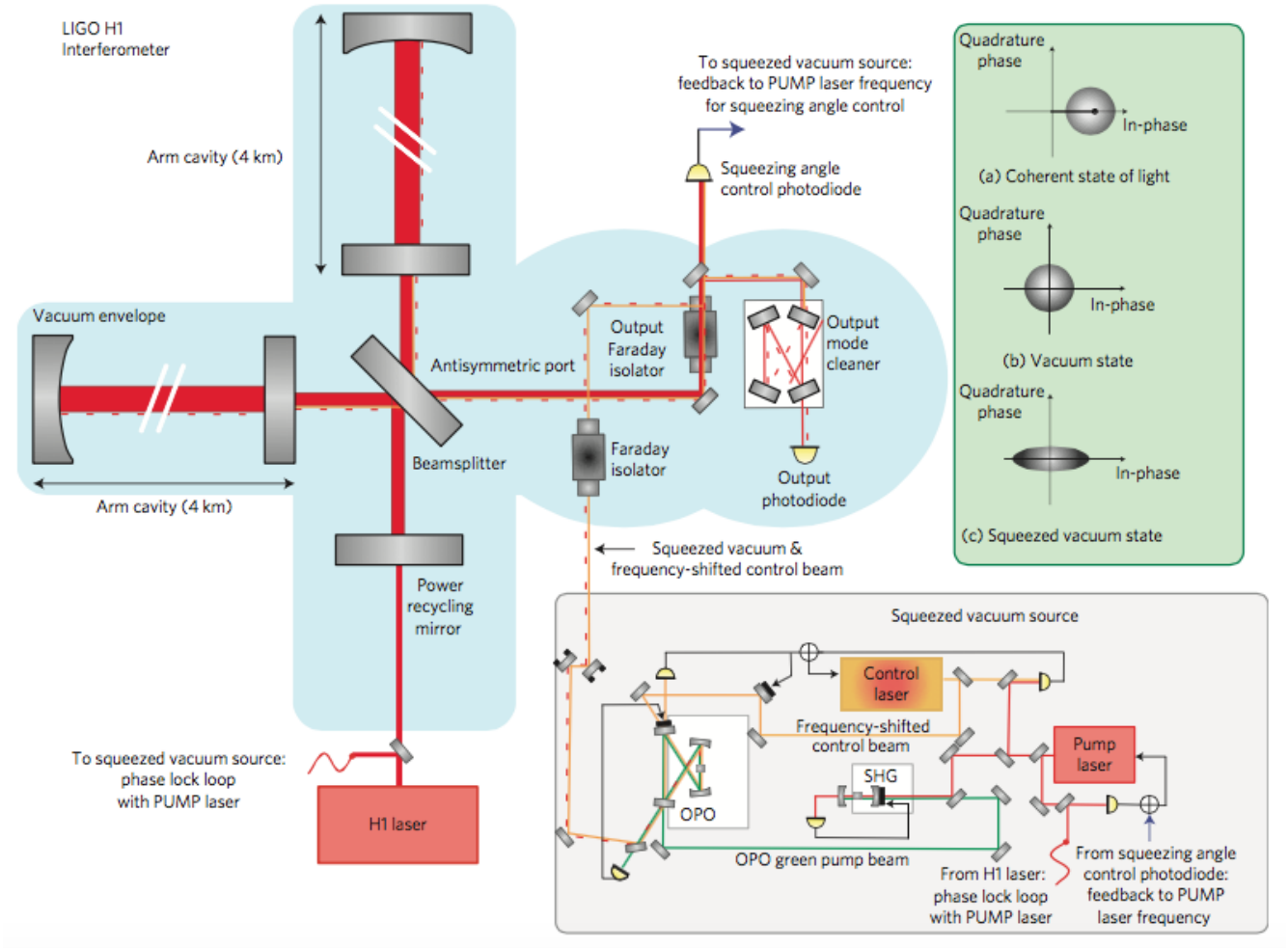

Figure 1: Squeezer in LHO. Reproduced from [1, Fig. 1].

2 Theory of Second Harmonic Generation

Harmonic generation is the hallmark of all nonlinear wave processes. Meaning, if you send in a monochromatic wave into a black box and waves of harmonic frequencies come out, we can say with certainty some nonlinear process occurred inside the box. Second Harmonic Generation is a special case of Sum Frequency Generation wherein two photons of the same frequency (interact with a nonlinear medium and) are combined into one photon of twice the original frequency. To gain a working understanding of SHG we need to look at Nonlinear Optics. The theory rests on the fact that the polarization response of a dielectric material to an applied electric field deviates slightly from linearity. This deviation becomes significant when the electric field reaches interatomic strengths, which lasers are capable of supplying [8, P.100]. To see how this works we assume the electric polarization response of a dielectric can be expressed as a Maclaurin Series (a reasonable assumption because the polarization should be continuous and differentiable are there any other requirements?) [8, Eq. 2.5]

$$\mathbf{P} = \epsilon_o \left(\chi^{(1)} \cdot \mathbf{E} + \chi^{(2)} : \mathbf{E}^{\otimes 2} + \chi^{(3)} \vdots \mathbf{E}^{\otimes 3} + \dots \right) \tag{8}$$

Where $\mathbf{E}^{\otimes n} = \mathbf{E} \otimes \mathbf{E} \otimes \dots$ is the tensor product of the electric field n times. Note the $1/n!$ coefficients have been absorbed into the $\chi^{(n)}$ susceptibility tensors. Equation 8 owes its complexity to its generality, but for our purposes it is unnecessarily general and we will work on simplifying it.

The first order term in equation 8 is the familiar linear susceptibility term which does things such as rotate the polarization and rotate the phase of each component of the electric field. Devices such as lenses, mirrors, polarizers, quarter wave plates, and half wave plates are linear devices. The second order term in equation 8 is the one of

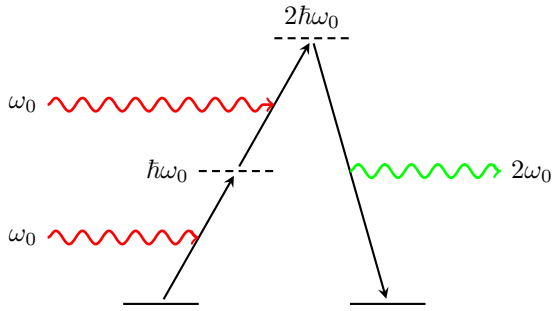

Figure 2: Energy level diagram of Second Harmonic Generation process.

interest in this paper. It is responsible for exotic optical processes such as Second Harmonic Generation, Sum and Difference Frequency Generation, and Optical Parametric Oscillation (a form of downconversion and source of squeezed light). To see how this one term can give rise to such a rich set of phenomena we write it in an equivalent way using an *effective SHG coefficient* $\mathbf{d_{il}}$ [8, Eq. 6.32] [**?**].

$$\mathbf{P^{(2)}} = \epsilon_0 \begin{pmatrix} d_{11} & \dots & d_{16} \\ d_{21} & \dots & d_{26} \\ d_{31} & \dots & d_{36} \end{pmatrix} \begin{pmatrix} E_x^2 \\ E_y^2 \\ E_z^2 \\ 2E_yE_z \\ 2E_zE_x \\ 2E_xE_y \end{pmatrix} \tag{9}$$

The first subscript i indicates the direction the medium will be polarized in by applying an electric field in the directions indexed by l. Generally one of the matrix elements will be much larger than the others. Appendix A gives an explanation how the jump from equation 8 to 9 was made. The effective SHG coefficient is often referenced in literature on the subject. Manufacturers always specify these values for their product because of how critically important it is to the operation of an SHG.

If we plug the electric field for a photon into this equation we obtain

$$\widetilde{\mathbf{P}} = \widetilde{\mathbf{P}}_{\mathbf{0}}^{(\mathbf{1})} e^{-i\omega t} + \widetilde{\mathbf{P}}_{\mathbf{0}}^{(\mathbf{2})} \left(1 + e^{-2i\omega t}\right) \tag{10}$$

This result is also taken from Appendix A. This is the polarization (up to second order) expressed as a fourier series. We can see the original wave survives, in addition to a constant term (0Hz) called optical rectification, and the second harmonic term.

This is obviously a classical description. If you were to interpret the above equation Quantum Mechanically, then you would find that sending a single photon of energy $\hbar\omega$ into the nonlinear medium you would get half a photon out of energy $2\hbar\omega$. This is not physically realistic because half a fundamental quantum of energy is nonsense.

To get an intuitive picture of Second Harmonic Generation we will start by considering it in terms of Quantum Mechanics. Refer to figure 2. Let's say we have two photons of angular frequency ω_0 that we wish to combine. In the nonlinear crystal there are two virtual energy levels (represented by dashed lines) both spaced $\hbar\omega_0$ apart. Both of the photons of energy $\hbar\omega_0$ interact with the nonlinear material kicking it up two virtual energy levels. Now there are two ways the system can relax, ether by stimulated or spontaneous emission. Ideally another second harmonic photon would stimulate the emission, and just like a laser the exiting light would be coherent. Unfortunately virtual energy levels are short lived, so the emission is spontaneous leaving no guarantee the second harmonic light will be coherent; an idea we will revisit. Either way when the system does relax it falls back to a real energy level (solid line) releasing the energy of both photons as one quanta of energy $\hbar(2\omega_0)$. Thus the frequency of light has been doubled.

From this picture we see SHG is a two photon process, which underscores the point that two photons need to interact simultaneously with the medium in roughly the same location in order to be combined into one photon of twice the energy. A higher photon density means two photons are more likely to be combined. Qualitatively we would expect conversion efficiency to increase as the intensity of incident light increases. Additionally we would expect there to be a saturation level for a real world SHG medium, so conversion efficiency should decrease (while converted power remains constant) as power increases beyond saturation.

A mathematical expression for output power as a function of intensity can be found by solving the non-linear wave equation with depletion. The exact non-linear wave equation reads

$$\left[\nabla^2 - \epsilon_0\mu_0(1+\chi^{(\mathbf{1})})\partial_t^2\right]\mathbf{E} = \mu_0\partial_t^2\mathbf{P_{NL}} + \mu_0\partial_t\mathbf{J_f} + \frac{1}{\epsilon_0}\nabla\rho_f - \frac{1}{\epsilon_0}\nabla(\nabla\cdot\mathbf{P}) + \mu_0\partial_t\nabla\times\mathbf{M} \tag{11}$$

Assume there are no free charges or currents and that magnetization effects are small all the terms in red are usually dropped. Plugging in a monochromatic and coherent plane wave traveling in the z direction into the nonlinear wave equation, and making many additional assumptions and approximations (the polarization is only second order in E, make the slowly varying amplitude approximation, dropping all waves of frequency other than the pumping and second harmonic, and reducing the effects of the linear susceptibility tensor down to only allowing the indices of refraction to be different in each direction) we can split the wave equation into two. These are the coupled non-linear wave equations:

$$\frac{\partial E_i^{(2\omega)}(z)}{\partial z} = \frac{i2\omega}{cn_i^{(2\omega)}}e^{-i\Delta kz}\mathbf{d_{il}}E_j^{(\omega)}(z)E_k^{(\omega)}(z) \tag{12}$$

$$\frac{\partial E_i^{(\omega)}(z)}{\partial z} = \frac{i\omega}{cn_i^{(\omega)}}e^{i\Delta kz}\mathbf{d_{il}}E_j^{(\omega)}(z)E_k^{(2\omega)}(z) \tag{13}$$

These are the equations that determine how energy is exchanged through $\chi^{(2)}$ between the different waves. The implications of the $\Delta k = k^{(2\omega)} - 2k^{(\omega)}$ term are so important that the whole next section is dedicated to investigating its effects.

3 Phase Matching and Temperature Tuning

The exact solution to the coupled wave equations for the evolution of the wave amplitudes in a lossless, non-linear medium is a Jacobi Elliptic Function sn [6]. From which an exact expression for the second harmonic power produced can be easily found. Here we present this in equation 14 as normalized power or equivalently as the efficiency $\eta = P_{2\omega}/P_\omega$.

$$\eta = \nu_b^2 sn^2\left(\frac{\Gamma L}{\nu_b}, \nu_b^4\right) \tag{14}$$

where Γ is the non-linear drive [7] and in the context of elliptic functions ν_b^4 is the elliptic modulus

$$\Gamma \equiv i\frac{\omega E_\omega^2}{n_{2\omega}c} \tag{15}$$

$$\nu_b = \left[\frac{\Delta k}{4\Gamma} + \sqrt{1+\left(\frac{\Delta k}{4\Gamma}\right)^2}\right]^{-1} \tag{16}$$

One important feature which is not obvious upon first glance of this solution is that efficiency increases with increasing input power. When there is perfect phase-matching so that $\Delta k = 0$ (or in the limit when the coherence length is much longer than the non-linear crystal) the expression for harmonic production efficiency reduces to

$$\eta(\Delta k = 0) = \tanh^2(\Gamma L) \tag{17}$$

where L is the length of the non-linear crystal [6]. This can be arrived at by solving the coupled equations and using conservation of energy (say something about depletion). The derivation can be simplified by assuming there is no depletion of the pump, which violates conservation of energy, but when conversion efficiency is low this is a good approximation. With some phase-mismatch and a low conversion efficiency corresponding to a small Γ the exact solution is commonly approximated as

$$\eta(\Gamma \to 0) \propto l_c^2 \sin^2\left(\frac{\pi l}{2 l_c}\right) \tag{18}$$

[8, Eq. 6.19] where l_c is the very important quantity known as *coherence length*, given by

$$l_c = \frac{\pi}{\Delta k} = \frac{\lambda}{4(n_{2\omega} - n_\omega)} \tag{19}$$

where λ is the free space wavelength of the fundamental [7, Eq. 2].

Here's where the phase-matching comes in. In a dispersive medium where $\Delta k \neq 0$ the fundamental and second harmonic have different phase velocities. The complex phase of $E_\omega^2 E_{2\omega}^*$ governs the relative phase between the fundamental and second harmonic [**?**]. As the phase angle between the waves rotates around, energy is exchanged back and forth and the direction of energy flow is controlled by this angle. The lagging wave gains energy from the leading wave and maximum energy is transferred when the waves are out of phase by $\pi/2$. Perfect phase matching ensures the second harmonic always lags behind the fundamental by $\pi/2$ leading to a constant and maximal energy transfer [6].

Given the phase determines the direction of energy flow, upon examining the plot of equation (????) in figure (????) we can see the coherence length is related to phase. At first all energy is in the pump and the second harmonic lags the pump by $\pi/2$. In the first coherence length energy is flowing monotonically into the second harmonic. At exactly one coherence length the roll is reversed; the second harmonic is at maximum intensity, the pump lags the second harmonic by $\pi/2$, and energy flows monotonically back into the pump. After two coherence lengths all energy has flowed back into the tonic. Physically the coherence length gives how long a non-linear crystal should be if it is to be used for second harmonic generation.

Phase matching can be realized in a variety of ways. If the material is birefringent the crystal can be angle tuned which exploits the difference in indices of refraction to achieve equal phase velocities. There is also Quasi-Phase Matching (QPM) which is controlled via temperature tuning. Second harmonic generation is only possible in non-centrosymmetric crystals, meaning the crystal lattice is non-isotropic. Periodically polling the crystal makes use of this non-centrosymmetry by flipping the crystal lattice periodically in layers running down the optic axis. Doing so has the effect of periodically reversing the sign of the effective SHG coefficient. QPM can also be done by interrupting harmonic generation by spatially alternating layers of linear and non-linear material. In the linear material the waves propagate until the phase is correct between them for harmonic generation.

A very interesting way to view quasi-phase matching is through momentum conservation. The phase matching condition is a statement of conservation of momentum. In a frequency doubling process where dispersion within the second order material results in a k-vector mismatch photon momentum is not conserved. By periodically polling the medium however, the difference in momentum is supplied by the wavevector of the periodic structure. Restoring holy momentum conservation.

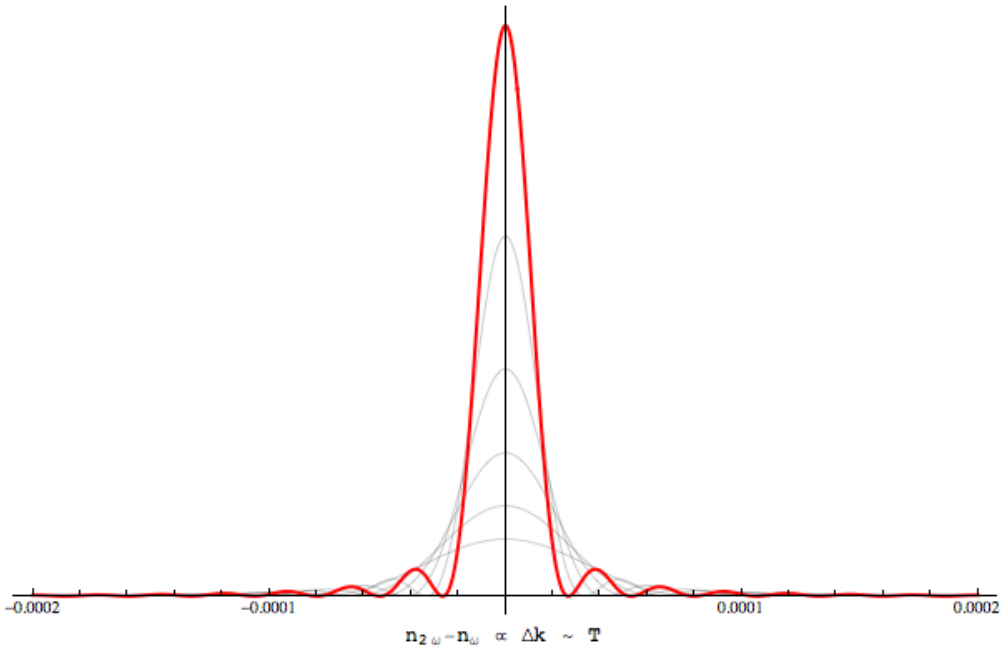

Figure 3: This plot shows the approximate temperature dependence of efficiency for a quasi-phasematched crystal. The various curves are for crystals of different length. As the crystals get longer, the maximum efficiency increases and the temperature curve gets sharper. It follows that temperature tuning becomes more important as the length of the crystal grows. At some point the accuracy to which you can control the temperature puts a limit on how of a crystal can be used. This plot was generated by graphing equation 14. Equation 19 was used to make equation 14 a function of the difference in indices of refraction for the two wavelengths. The red curve is for a 1cm long crystal. The fundamental wavelength is 1064nm.

4 Conversion Efficiency, Power Recycling, and Fabry-Perot Cavities

As previously mentioned nonlinear effects are small. It is this property which allows us to write the polarization as a power series as in equation 8. We can maximize the effect by using some sort of phase matching, but even still the effects are vanishingly tiny. One way to boost the effect would be to use a longer crystal. The longer the crystal becomes though the more precise the phase matching needs to be. Remember the coherence length puts an upper bound on how long the crystal can be. In practice one cannot simply pass a laser beam through a nonlinear crystal and expect any appreciable amount of harmonic power out. The effective SHG coefficient is just too small. To increase efficiency to a practical level the unconverted light needs to be recycled back through the crystal many times. Moreover all light passing through the crystal needs to be in phase so as to interfere constructively.

The perfect solution is to place the SHG crystal in a Fabry-Perot Cavity. A Fabry-Perot Cavity is a type of optical resonator consisting of two partially reflecting mirrors which allow power to build up between them. Such a cavity is often called a standing wave resonator because in steady state operation waves are traveling in both directions; the criteria for standing waves [9, P.412]. The amount of power transmitted, reflected, and buildup inside the resonator are all a function of cavity length. Power buildup is greatest inside the cavity when transmitted power is at a maximum. This is because the power transmitted through the second mirror (and the cavity) is proportional to the amount of power incident upon the second mirror (i.e. resonating in the cavity). Using the Pound-Derver-Hall method we tune the cavity length so transmitted power is held at a maximum, ensuring maximal coherent power build up which in turn results in maximum conversion efficiency.

Here's an overview of some important terms that get thrown around a lot in an experiment involving a Fabry-Perot cavity. The *complex round-trip gain* (in the next section we will call this an eigenvalue) tells how the phase and amplitude of the wave change after one round trip.

$$\widetilde{g}_{rt}(\omega) \equiv (r_1 \cdot r_2 \cdot \dots)\rho e^{-i\delta} \tag{20}$$

Where ρ is the round-trip gain or loss due to any medium inside the cavity (the SHG crystal) and δ is the accumulated round-trip phase [9, Eq. 11.18].

Waves of certain frequencies naturally resonate in a Fabry-Perot cavity based on it's length. These resonant modes are known as the axial-modes of the cavity, which occur when $\delta \equiv 0(\mod 2\pi)$:

$$\omega_{ax} = \frac{2\pi c q}{p}; q \in Z \tag{21}$$

where $p \geq 2L$ is the distance a beam of light travels in one round trip and L is the cavity length. The spacing between axial-mode resonances, known as the axial-mode spacing or free-spectral range, is [9, Eq. 11.47]

$$\Delta\omega_{ax} = \frac{2\pi c}{p} \tag{22}$$

In this experiment the wavelength was held constant and the length of the cavity changed to match it. Rearranging equation 22 indicates $L_{ax} = \frac{1}{2}q\lambda$, or the cavity is in resonance when it is a half wavelength multiple of the light long. Another useful quantity is the Full Width at Half Maximum (FWHM) Bandwidth $\Delta\omega_{cav}$. It is defined as the width of the resonance peak (in angular frequency) at half its maximum value. This gives an effective measure of how sharp the resonance peak is [9, Eq. 11.52].

$$\Delta\omega_{cav} = \frac{4c}{p}\arcsin\left[\frac{1-g_{rt}(\omega)}{2\sqrt{g_{rt}(\omega)}}\right] \approx \frac{1-g_{rt}(\omega)}{\pi\sqrt{g_{rt}(\omega)}} \times \Delta\omega_{ax} \tag{23}$$

Similar to bandwidth is Finesse. When the round trip gain is roughly unity, finesse is approximately the axial-mode spacing divided by FWHM bandwidth; it becomes something like the inverse of scaled bandwidth [9, Eq. 11.54].

$$F \equiv \frac{\pi\sqrt{g_{rt}}}{1-g_{rt}} \approx \frac{\Delta\omega_{ax}}{\Delta\omega_{cav}} \tag{24}$$

All of these quantities are really describing various aspects of the reflection and transmission coefficients which are given below and graphed as a function of frequency in figure 4.

	E Field (General Form)	E Field (For a 2 Mirror FP Cav.)	Power (For a 2 Mirror FP Cav.)
Reflected	$r_c = r_1 - \frac{t_1^2\widetilde{g}_{rt}}{r_1(1-\widetilde{g}_{rt})}$	$r_c = r_1 - \frac{t_1^2 r_1\rho e^{-i\delta}}{1-r_1r_2\rho e^{-i\delta}}$	$R_c = \lvert r_c\rvert^2$
Transmitted	$t_{c,x} = \frac{t_1t_x}{\sqrt{r_1r_2\ldots}} \times \frac{\sqrt{\widetilde{g}_{rt}}}{1-\widetilde{g}_{rt}}$	$t_c = \frac{t_1t_2\sqrt{\rho}e^{-i\delta/2}}{1-r_1r_2\rho e^{-i\delta}}$	$T_c = \frac{T_1T_2}{1+R_1R_2-2\sqrt{R_1R_2}\cos(2\delta)}$
Buildup	$b_c = \frac{t_1}{\sqrt{r_1r_2\ldots}} \times \frac{\sqrt{\widetilde{g}_{rt}}}{1-\widetilde{g}_{rt}}$	$b_c = \frac{t_1\sqrt{\rho}e^{-i\delta/2}}{1-r_1r_2\rho e^{-i\delta}}$	$B_c = \frac{T_1}{1+R_1R_2-2\sqrt{R_1R_2}\cos(2\delta)}$

Table 1: The notation t_x means t for the x^{th} mirror, and $t_{c,x}$ denotes the transmission coefficient of the cavity through the x^{th} mirror. R_c is given in its simplest form. [9, Eq. 11.27, 11.29]

Sometimes it is convenient to express the transmissivity of the cavity in terms of the finesse [9, Eq. 11.53]

$$T_c = \frac{T_{max}}{1+(2F/\pi)^2\sin^2(\delta)} \tag{25}$$

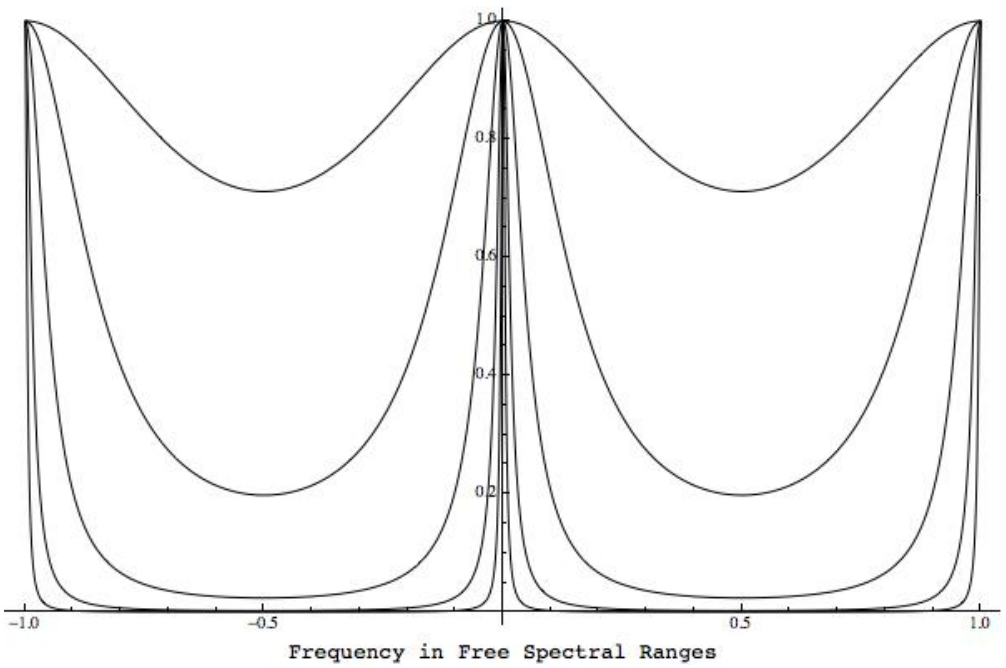

Figure 4: Normalized transmissivity of a Fabry-Perot cavity plotted for finesses ranging from 10^0 to 10^2 where the exponent is incremented in steps of 0.5.

Resonant power is maximized for an *impedance matched cavity*. In this special case the reflectivity of mirror one R_1 equals the effective reflectivity of the rest of the cavity $\rho^2 R_2$, and at resonance the reflection coefficient of the cavity R_c vanishes. This is analogous to impedance matching in tuned circuits [9, P.423]. Obviously it is desirable to impedance match the two mirrors with the harmonic generation losses then. This is not easily done, as second harmonic conversion efficiency depends on, amongst other things, the intensity of light in the cavity. This means η is a function of power. One could tune the waist size by adjusting cavity length, since waist size determines intensity which in turn determines η. For a symmetric cavity the waist will be located at the center, and the size of the waist is given by [5, Eq. 48]

$$w_0 = \sqrt{\frac{\lambda}{2\pi}\sqrt{d(2R-d)}} \tag{26}$$

However there is not an indefinite amount of dynamic range in the waist size. Any two mirrors can be used to construct a Fabry-Perot Cavity but in general they will not form a stable resonator. Condition for a stable resonator consisting of two spherical mirrors is given by [5, Eq. 8] :

$$0 < \left(1 - \frac{d}{R_1}\right)\left(1 - \frac{d}{R_2}\right) < 1 \tag{27}$$

where R is the radius of curvature of that spherical mirror, and d is the distance separating both mirrors. Kogelnik and Li have a beautiful graphic summarizing stable resonators which is reproduced in figure 5.

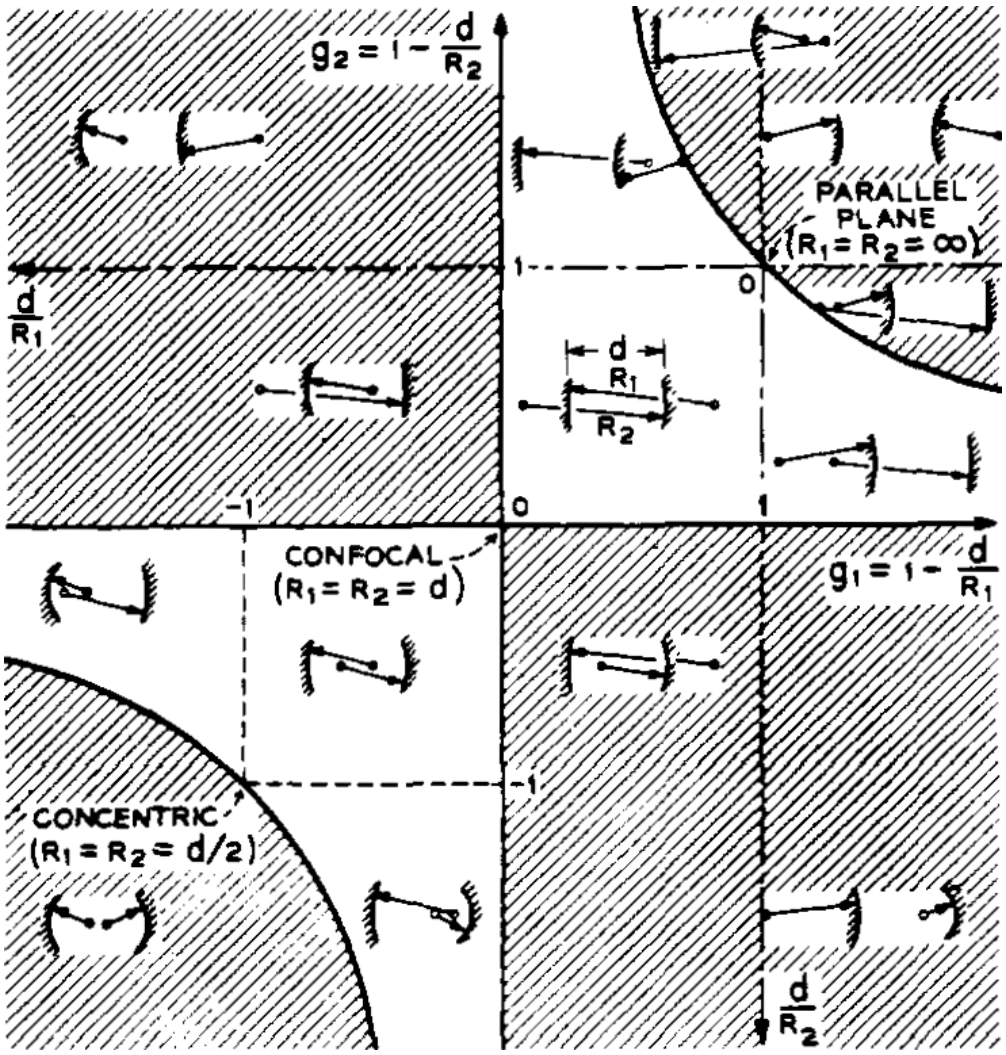

Figure 5: Stability of optical resonators. Image credit: Kogelnik and Li [5, Fig. 4]

(Could this be another consideration for what type of cavity should be used. impedance matching depends on conversion efficiency which depends on waist size depends which depends on cavity length)

With perfect phase matching in the nonlinear crystal $k_{2\omega} = 2k_{\omega}$. This unavoidable condition means when the pumping frequency is in resonance the second harmonic will ether be perfectly resonant, or as far from a resonance as possible. In the case where both are resonant, the second harmonic builds up inside our resonator, subjecting it to the same losses the pumping wave experiences due to harmonic generation. The simplest resolve is to make the cavity a resonator for just the pumping frequency. This is accomplished by using dichroic mirrors. A summery the Fabry-Perot optics used are given in table 2.

	T for 1064 nm (532 nm)	R for 1064 nm (532 nm)	Mirror Radius of Curvature	Lens Radius of Curvature
M1	(HT)	90 %	20 mm	25 mm
M2		99.85 % (HR)	20 mm	25 mm

Table 2: Summery of Optics used inside the SHG. Both optics are 1/2 inch in diameter. HT - High Transmit. HR - High Reflect.

The mirrors are actually quite fancy. On top of being dichroic and specially reflective they are spherical and have lenses built in for focusing the beam. The conversion efficiency of the crystal is directly related to the intensity of light, so in general a smaller, more focused beam is better. There are other things to consider which is touched

upon in section (????).[1]

5 Transverse Cavity Modes

In the preceding section we discussed axial modes. This section will give a overview of the transverse modes, which can be thought of as describing the cross-section of a beam. The field distribution of a laser beam is often approximated as a Spherical-Gaussian Wave given by equation (???). In free space the spherical-gaussian mode is, by definition, the lowest order mode solution to the paraxial wave equation because it is the least spatially diffuse. A brief and somewhat contrived derivation is given in Appendix C as it is pertinent to the following discussion of cavity modes.

$$\widetilde{\mathbf{\Upsilon}}(s,z) = \widetilde{\mathbf{\Upsilon}}_{\mathbf{0}} \frac{1}{\widetilde{q}(z)} \exp\left[-i\frac{ks^2}{2\widetilde{q}(z)}\right] \tag{28}$$

Determining the eigenmodes for the electric field inside a closed cavity with lossless walls is a familiar procedure. The wave equation is solved in the favored coordinate system if symmetry prescribes one, then boundary conditions are applied to find the eigenmodes. In instances like these the wave equation describing the cavity field is a hermitian operator; meaning the eigensolutions form a complete orthogonal basis set of functions with real (no phase shift) eigenvalues. Any field distribution can exist in the cavity due to the completeness of the solution set.

Finding the eigenmodes of open optical resonators proves to be much more mathematically difficult problem. Namely the wave equation is usually not a Hermitian operator. The important implication being, not every arbitrary field distribution within the cavity can resonate because generally there is not a complete set of orthogonal functions with which the distribution can be expressed in terms of.

To find the eigenmodes of a cavity consisting of two finite spherical mirrors assume that some chunk of beam inside the cavity and bounces around, making one round trip. For the time being let's omit the SHG crystal from the discussion; in practice it doesn't appreciably change the shape of the modes. The new equation for the transverse distribution of the chunk is given by [9, Eq. 14.2]

$$\mathbf{E}^{(\mathbf{n+1})}(x,y) = e^{-ikp} \iint_{z_0} \widetilde{K}(x,y,x_0,y_0)\mathbf{E}^{(\mathbf{n})}(x_0,y_0)dx_0dy_0 \tag{29}$$

Where $p \geq 2L$ is the round trip distance of the mode, and K is called the round-trip propagation kernel. The subscript of z_0 on the integral indicates the inner product of $\widetilde{K}$ and $\mathbf{E}^{(\mathbf{n})}$ should be evaluated at some plane inside the cavity. The superscript on $\mathbf{E}$ gives the number of times the chunk has crossed the z_0 plane. Once the axial-phase $\exp[-ikp]$ has been factored out, the linear operator depends very little on the actual wavelength. Physically this can be explained by realizing diffraction effects are the significant contributor to the propagation kernel's wavelength dependence. Variation in the diffraction effects across wavelengths, especially within the bandwidth of an atomic transition generating a laser beam, are small. This affords us the luxury of being able to consider transverse and axial modes separately [9, P.569].

Special beam distributions retain their shape. Distributions with this property are the eigenmodes of the cavity which satisfy [9, Eq. 14.4]

$$\widetilde{\gamma}_{\mu\nu}\mathbf{E}_{\mu\nu}(x,y) = e^{-ikl} \iint_{z_0} \widetilde{K}(x,y,x_0,y_0)\mathbf{E}_{\mu\nu}(x_0,y_0)dx_0dy_0 \tag{30}$$

The subscripts $\mu\nu$ index the eigenfunctions. It is important to note the distinction between eigenmodes and resonant modes. Resonant modes accumulate a phase difference of $0(\mod 2\pi)$ over the course of one round trip through the cavity, but we make no requirement as to their transverse shape. Whereas eigenmodes retain their shape through one round trip, but no stipulation is given regarding the phase. Eigenmodes can be resonant (and if the propagation kernel was hermitian, every eigenmode would be resonant ???). Here the eigenmode is multiplied by a possibly complex eigenvalue, meaning it can acquire a phase shift. Comparing these two equation we obtain how the eigenfunctions evolve over time

$$\mathbf{E}^{(\mathbf{n})}_{\mu\nu}(x,y) = (\widetilde{\gamma}_{\mu\nu})^n \, \mathbf{E}^{(\mathbf{0})}_{\mu\nu}(x,y) \tag{31}$$

[1] For further reading sections 11.2-11.5 in Lasers by Siegman are simply excellent.

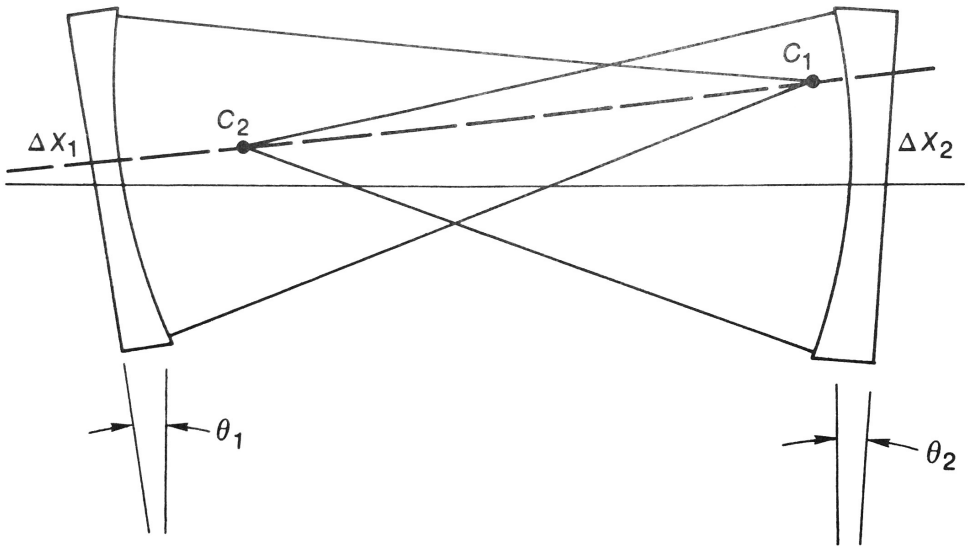

Figure 6: Perturbed optical axis (dashed line) of resonator with misaligned spherical mirrors. Image credit: [9, Figure 19.18]

So all the dynamics of the eigenmodes are determined by the eigenvalues. The normalized power of the eigenmode after n passes through the cavity is $1-|\widetilde{\gamma}_{\mu\nu}|^{2n}$. Without knowing any specific information regarding the propagation kernel we can actually construct the eigenvalue. First note we can write the eigenvalue in the form $\widetilde{\gamma}_{\mu\nu} = |\widetilde{\gamma}_{\mu\nu}|\, e^{i\phi}$. Reflection at a mirror multiplies the wave by a reflection coefficient. Then there is some loss due to the finite size of the mirrors and the SHG crystal acting as an aperture. By definition different modes have different spacial distributions, so this loss, call it $\eta_{\mu\nu}$, will be a function of the mode. (Additionally there is a replenishing term due to an external laser pumping the cavity which can be absorbed into $\eta_{\mu\nu}$) As for the phase accumulated, obviously there is a kp term associated with propagating some distance p. Then there is a phase change at each mirror. For most two mirror systems the effects of reflection at each mirror cancel, but by allowing the reflection coefficient to be complex it can carry a phase shift. Finally the Gouy Effect leads to a phase shift $\psi_{\mu\nu}$ that will be very important later on. Combining all these factors the eigenvalue reads

$$\widetilde{\gamma}_{\mu\nu} = r_1 r_2 \eta_{\mu\nu} e^{i(\psi_{\mu\nu} - kl)} \tag{32}$$

5.1 Cavity Misalignment and Higher Order Transverse Modes

Breaking the symmetry of a cavity by having off axis elements in an experimental setup further complicates the field distribution within a resonant cavity. Theoretically proving transverse eigenmodes even exist is extremely difficult, but it empirically obvious such modes do build up in real resonators [9]. Though the problem is complex, a simple argument for the shape of these modes is presented here.

The axis of symmetry of a resonator should have the property of preserving the symmetry of a ray of light traveling along it; i.e. the ray should always lie on this axis. For spherical mirrors, a line passing through the center of curvature is normal to the surface where it intersects the mirror. An intuitive definition of the optical axis for a resonator, then, is the line that passes through the center of curvature of each spherical mirror; see figure 6 [9, P.768]. Tilting and translating mirrors have the effect of rotating and translating the optical axis. For a near concentric resonators the centers of curvature lie very close to each other, and any perturbation in alignment will wildly rotate the optical axis. Hence these types of resonators are very susceptible to destabilization due to alignment defects [9, P.756]. In general as $g_1 g_2 \to 1$ the sensitivity to misalignments blows up [9, P.769].

When the laser beam and resonator don't share the same axis the symmetry of the system is reduced. Imagine the laser beam and resonator axes are coplanar and distinct, i.e. they both lie in say the x-z plane, but they are not the same line. Then the system is still symmetric about this plane. Assume this reduction of symmetry has the effect of adding an x dependence into the field distribution. (THis might not be quite right. The solutions are symmetric about x and y) We are looking for a solution that modifies the lowest order – Spherical-Gaussian mode $\widetilde{\Upsilon}$; something of the form: [5, Eq. 30]

$$\widetilde{\mathbf{u}} = H_\mu \left(\frac{x}{w}\right) \widetilde{\boldsymbol{\Upsilon}} \tag{33}$$

Inserting this into the paraxial wave equation (equation no.?) one finds H_μ satisfies the differential equation for the Hermite Polynomials. If the axes are skew (non-coplanar) then even the symmetry about the plane is lost, so we introduce a y dependence. Following the same proscription outlined for x one finds the y dependence to also be a Hermite Polynomial. The elegant Hermite-Gaussian modes are given by [9, Eq.16.67]

$$\widetilde{\mathbf{u}} = \widetilde{\mathbf{u}}_\mathbf{0} \left(\frac{\widetilde{q}_0}{\widetilde{q}(z)}\right)^{\nu+\mu+1} H_\mu \left(\sqrt{\frac{ikx^2}{2\widetilde{q}(z)}}\right) H_\nu \left(\sqrt{\frac{iky^2}{2\widetilde{q}(z)}}\right) \exp\left[-i\frac{k(x^2+y^2)}{2\widetilde{q}(z)}\right] \tag{34}$$

Some of the lower order Hermite-Gaussian modes are shown in figure 8a. Hermite-Gaussian modes are the eigenmodes of the paraxial wave equation in Cartesian Coordinates in free space. So when there is a some sort of symmetry in the problem that demands cartesian coordinates this is the natural solution set to go with. They are not the exact eigenmodes of the cavity, but in practice they approximate them well, and because they are complete the true modes can be expressed as a linear combination of them. A word of warning, these solutions are not orthogonal outright, they are biorthogonal with an adjoint set of hermite polynomials [9, P.650] [**?**]. (they are only orthogonal with respect to a gaussian weighting function [**?**].)

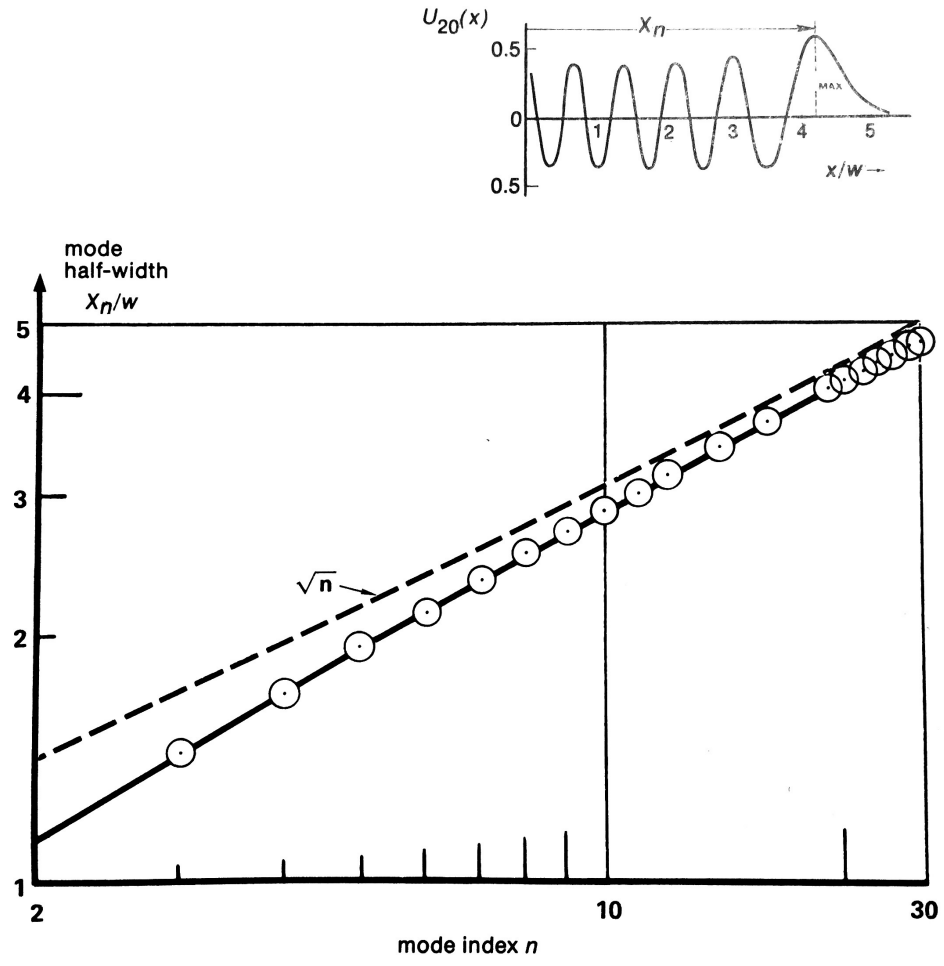

Figure 7: Reproduced from Seigman figure 17.23 [9, Fig. 17.23].

It is an empirical fact that resonators prefer to resonate in the Hermite-Gaussian Modes over other modes species. (Why?) Interestingly the SHG has a bias for resonating in lower-order modes. Referring to figure 7 the

position of the brightest spot corresponding to the global maximum of the polynomial is also the farthest from center. This makes the location of the brightest spot an effective measure of the half width of the mode which roughly goes as $w\sqrt{n}$ [9, Eq. 17.44]. The higher order modes are, by definition, more spatially diffuse causing them to be more susceptible to diffraction losses. Fractionally more power is lost in higher order modes because a higher portion of the energy misses the mirrors altogether and gets blocked by the aperturing effect of the SHG crystal mount. The SHG has an attenuating effect on higher order modes. However this does not mean the most prominent mode in the cavity is always the Spherical-Gaussian. The loss of symmetry causes the cavity to favor a higher modes, while attenuating very high modes.

5.2 Input Mode Matching and Higher Order Longitudinal Modes

Using the same simple symmetry argument we can arrive at a different complete solution set for the paraxial wave equation in free space. This time assume the axial symmetry is preserved. While it is still possible to express any field distribution within the cavity as a linear combination of the Hermite-Gaussian modes because they form a spanning set over hilbert space, it will be awkward to do so because they do not share the same symmetry as the system. To find a more natural solution set to express higher order modes in cylindrically symmetric problems assume there is some angular and radial dependence. Using a envelope of the form

$$\widetilde{\mathbf{u}} = L_p\left(\frac{r}{w}\right) e^{-im\phi}\widetilde{\boldsymbol{\Upsilon}} \tag{35}$$

as a test function we plug it into the paraxial wave equation and find it satisfies the differential equation for the Laguerre Polynomials.

——— Eq. 16.64 ? ———

Laguerre-Gaussian modes are for paraxial and Bessel are for true wave eqn?

It is not as obvious how these modes arise in a physical system.

To see how a higher order mode could be excited in a perfectly aligned cavity we need to see how this differs from lowest order mode resonance, the condition for which is:

At the location of ether mirror, the radius of curvature of the
Spherical-Gaussian wave must equal the radius of curvature of that mirror.

This ensures the beam retains its shape because it is reflecting off a surface that is parallel to the wave front. (it shape and satisfies the eigenequation (eqn. no.?)). (Also this gives the wavepacket-resonator system time reversal symmetry.) Knowing the radius of curvature at two points determines the size which is given by equation 26 which should be located at the center for a symmetric cavity. When the laser beam pumping the cavity does not exactly satisfy these conditions higher order longitudinal modes arise. The process of transforming the pumping beam into the lowest order eigenmode of the cavity is called mode matching. In practice this is done with an array of lenses. One procedure for accomplishing this is given in the Tuning section.

As with the transverse modes, the higher order longitudinal modes are more spatially diffuse, making them susceptible to the same losses the transverse modes succumb to due to

There is one caveat regarding higher order modes that deserves mention. In special cases a higher order transverse mode can look like a longitudinal mode and vise versa. Both the transverse and longitudinal solution sets are complete, so an element of one set can be constructed from elements of the other. A very commonly encountered example is the Doughnut Mode. It looks like it should be a longitudinal mode mismatch indicator, but really it is a simple superposition of 10 and 01 Hermite-Gaussian modes. Correcting a longitudinal mode mismatch is an intensive process which can take days, where as transverse misalignments are relatively easy to fix. Not recognizing a mirror misalignment can result in days of adjusting lenses.

Also worth noting, in the laboratory resonator mirror misalignments and improperly mode matched input beams are not mutually exclusive. Reflecting this fact, nether are higher order transverse and longitudinal modes. They are both solutions to the paraxial wave equation so there is no reason the resonator modes cannot be simultaneous eigenfunctions of both. Though in practice transverse modes are easier to excite [9, P.688] and once the pumping beam is decently mode matched to the cavity higher order longitudinal modes simply reflect off the cavity (is this true?)

So why allocate so much of this paper to a discussion of modes? Because they directly effect the efficiency of the SHG.

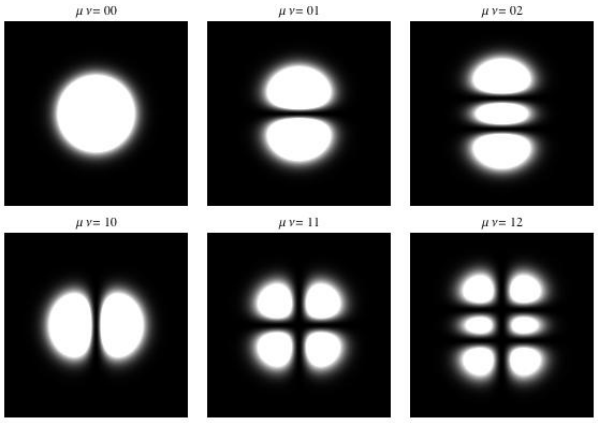

(a) Hermite Gaussian Modes. The 00 mode is the Spherical-Gaussian.

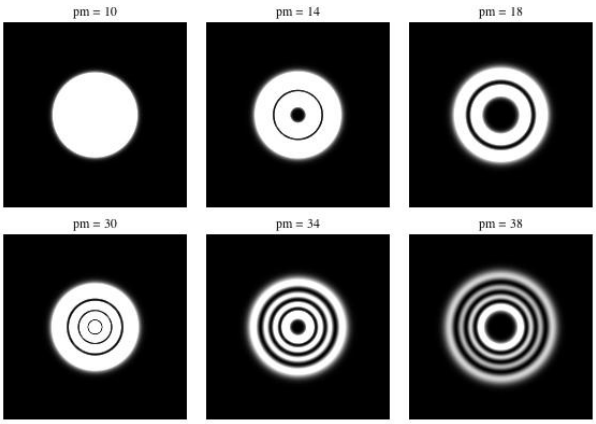

(b) Laguerre Gaussian Modes

5.3 Beating of Cavity Modes

Earlier on we said axial and transverse mode can be treated separately. This is not entirely the case. As mentioned in the ????? section, the condition for an axial mode resonance is the mode must accumulate a total phase of 0(mod 2π). The act of focusing a beam actually introduces a phase shift which the beam picks up as it passes through the waist. This is known as the Guoy Effect. For a gaussian spherical beam the phase shift is

$$\psi(z) = \arctan\left[\frac{\lambda(z - z_0)}{\pi w_0^2}\right] \tag{36}$$

in the limit $|z - z_0| >> \pi w_0^2/\lambda$ the phase shift is $\psi \approx \pm\pi/2$, and the total phase shift due to focusing a spherical gaussian is π. The Guoy Effect is different for higher order modes.

$$\psi_{\mu\nu} = (\mu + \nu + 1)\psi \tag{37}$$
$$\psi_{pm} = (2p + m + 1)\psi \tag{38}$$

[9, P.685] [5, Eq. 39] The consequence of the Guoy Effect for a resonator containing a waist, is that different transverse modes *may* have different resonant frequencies. For a perfectly confocal cavity axial modes are perfectly degenerate for each transverse mode [9, P.439]. Perfectly confocal cavities also have the added benefit of being relatively forgiving of misalignments, and are difficult to excite higher order modes in.

Let gamma be the eigenvalue of a mode.

The total phase accumulated for a round trip is $kp + \psi_{\mu\nu}$, and equating this to the resonance condition

$$kp + \psi_{\mu\nu} = 2\pi q \tag{39}$$

and using the relation $k = \omega/c$ we arrive at [9, Eq. 14.18]

$$\omega_{q\mu\nu} = \frac{2\pi c}{p}\left[q + \frac{\psi_{\mu\nu}}{2\pi}\right] \tag{40}$$

equate this to the total round trip phase for resonance condition, and note that k = omega/c
(2 omega l)/c + (phase angle of eigenvalue) = 2pi*n
solve for omega and also note that n = 2L/lambda so
omega = (pi*c)/(L) * (2L/lambda + (phase angle of eigenval)/(2pi))
[9, Eqn. 14.18]

There is something fishy here. lambda can also be expressed as a function of omega related by c (this is valid if the medium is homogenous and isotropic so the dispersion relation is the same for each mode) so shouldn't omega not be a function of lambda? something to think about

the difference in these mode frequencies are the beats.

this is a very sensitive way to determine if there are higher order modes present in the resonator.

What are the implication for LIGO?

Though this is a small effect, and for a properly mode matched and aligned SHG the effect disappears completely, but it does illustrate the importance of mode matching.

6 Pound-Drever-Hall

The aLIGO Optical Second Harmonic Generator uses a variation of the famous Pound-Drever-Hall method to bring the Fabry-Perot Cavity into resonance with the pumping laser beam. The conventional PDH technique was developed as a method for creating a laser beam that is as stable in frequency as a pulsar []. It accomplishes this by locking onto a Fabry-Perot reference cavity with a free spectral range that is more stable than the laser's frequency; an error signal is fed back into the laser as needed. Frequency stabilization techniques existed before PDH, but these methods could not distinguish between amplitude and phase noise. The PDH method's ability to decouple these two noise sources is what makes it so useful.

In our situation we do not have the luxury of being able to tune the laser frequency. The applications of the SHG in aLIGO require it to accept a beam which can vary slightly in frequency to produce the harmonic. This means the SHG has to dynamically tune the Fabry-Perot cavity to the pumping frequency. The PDH method can be easily adapted for this purpose.

Here an overview of the technique is given within the context of the experiment. Simply measuring the transmitted optical power through the Fabry-Perot cavity cannot determine which side of a resonance the cavity is on. As figure 4 shows, this quantity 25 is an even function about a resonance. However the derivative is an odd function, making it suitable for constructing an error signal which carries information about how far off resonance the cavity is. Note the value of the derivative scales with input power, but sign, not absolute value is what's important. The question becomes how to take the derivative of equation eqn: transmissivity and finesse?

The convention is to use the cavity's reflected light for PDH, but because we use transmitted light the math for this version of PDH is presented here.

First sinusoidally dither the pumping beam's frequency. This is done by passing the beam through an electro-optical phase modulator (EOM) driven by an RF synthesizer. It turns out phase modulating a wave is mathematically equivalent to frequency modulation. The Jacobi-Anger expansion gives the Fourier Coefficients of a phase modulated beam.

$$e^{i(\omega t+\beta\sin\Omega t)} = J_0(\beta)e^{i\omega t}+\sum_{n=1}^{\infty}\left(J_n(\beta)e^{i(\omega+n\Omega)t}+(-1)^nJ_n(\beta)e^{i(\omega-n\Omega)t}\right) \tag{41}$$

$$\approx J_0(\beta)e^{i\omega t}+J_1(\beta)e^{i(\omega+\Omega)t}-J_1(\beta)e^{i(\omega-\Omega)t} \tag{42}$$

[2, Eq. 3.2]

Generally only the first three terms are kept – the carrier and two sidebands. The electric field transmission coefficient t_c, given in table 1, is a function of frequency. So multiplying each frequency component by the appropriate transmission coefficient gives the transmitted electric field of a phase modulated beam through a Fabry-Perot cavity. This quantity is proportional to [2]

$$E_t(t)\propto J_0(\beta)t_c(\omega)e^{-i\omega t}+J_1(\beta)\left[t_c(\omega+\Omega)e^{-i(\omega+\Omega)t}-t_c(\omega-\Omega)e^{-i(\omega-\Omega)t}\right] \tag{43}$$

(More important than changing the amplitude, the transmission coefficient also shifts the phase one is even funct the other is odd?!) and the transmitted power is then [2, Eq. 3.3]

$$\begin{aligned}P_t(t)\propto{}& J_0^2(\beta)\left|t_c(\omega)\right|^2+J_1^2(\beta)\left(\left|t_c(\omega-\Omega)\right|^2+\left|t_c(\omega+\Omega)\right|^2\right)\\ &+2J_0(\beta)J_1(\beta)\Big[\Re\left\{t_c(\omega)t_c^*(\omega+\Omega)-t_c^*(\omega)t_c(\omega-\Omega)\right\}\cos\Omega t\\ &\qquad+\Im\left\{t_c(\omega)t_c^*(\omega+\Omega)-t_c^*(\omega)t_c(\omega-\Omega)\right\}\sin\Omega t\Big]\\ &-2J_1^2(\beta)\Re\left\{t_c(\omega-\Omega)t_c(\omega+\Omega)e^{-i2\Omega t}\right\}\end{aligned}$$

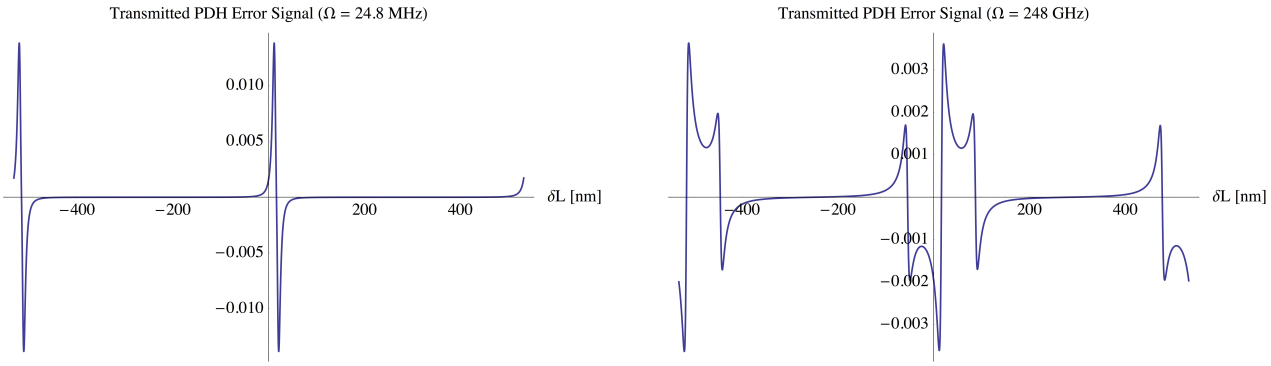

(a) **(b)**

Figure 9: These two plots show the transmitted Pound-Drever-Hall error signal for a Fabry-Perot cavity with a wavelength of 1064 nm. The error signal is an anti-symmetric function of cavity length. In this experiment we used a modulation frequency of 24.8 MHz (a). In figure (b) at a higher modulation frequency the PDH error signal looks like the classical. These plots shouldn't be shifted to the right of the origin; Mathematica wants to plot them this way for some reason.

This should be the signal at the highspeed photoreceiver. We then mix this signal with the signal from the synthesizer. A mixer takes the product of the two signals. Taking the product of two waves gives sum and difference frequencies.

$$\sin(\Omega t)\sin(\Omega t+\phi) = \frac{1}{2}[\cos(\phi) - \cos(2\Omega t+\phi)] \tag{44}$$

$$\cos(\Omega t)\sin(\Omega t+\phi) = \frac{1}{2}[\sin(\phi) + \sin(2\Omega t+\phi)] \tag{45}$$

After mixing, the only terms which will give a constant frequency are the ones in black. To isolate the constant term the output from the mixer is passed through a low pass filter. In our setup this was included in the SR-550 amplifier. It turns out the real part is an even function about a resonance, so we want to use the imaginary term. The cables labeled "delay line" in the electrical schematic 11 control the phase between the waves fed into the mixer. We want to adjust these so that the phase difference $\phi = \pm\pi/2$. This allows us to select only the imaginary term, optimizing the PDH method. If $\phi \equiv 0 \mod 2\pi$ then real part is selected and the PDH method completely breaks down. The length of these cables then is critical to the performance. The PDH error signal is

$$\propto J_0(\beta)J_1(\beta)\Big[\Re\left\{t_c(\omega)t_c^*(\omega+\Omega) - t_c^*(\omega)t_c(\omega-\Omega)\right\}\sin\phi + \Im\left\{t_c(\omega)t_c^*(\omega+\Omega) - t_c^*(\omega)t_c(\omega-\Omega)\right\}\cos\phi\Big] \tag{46}$$

again, we want to adjust ϕ so that the term in red disappears. This is amplified somewhere between 10^4 and 10^6 times, fed into a piezo driver, and then into the piezo which adjusts the cavity length.

7 Experimental Setup

Figure 10 below shows the optical experimental setup in its final form. Directly after the laser a half wave plate (HWP), polarizing beamsplitting cube (PBSC), and beamstop are used to attenuate the laser power. An optical diode is used after the attenuator system to prevent light from reentering the laser which can destabilize it. Another half-waveplate and polarizing beamspliting cube are used to divide the remaining power between two experiments. The s-polarized (electric field vertically polarized) light is used for this experiment. The light enters an electro-optical modulator (EOM) which phase modulates the light putting RF sidebands on the beam which is necessary for Pound-Drever-Hall. A pair of mirrors are used to bring the beam up from the height of the laser to the height of the SHG. The SHG crystal is sensitive to the polarization of light, so another half wave plate may be necessary somewhere before the SHG. A dichroic beamsplitter is used to separate the green and infrared light. The first four lenses are used for mode matching. The last pair of mirrors are used to lower the transmitted beam from the height of the SHG to the height of the photoreceiver, and the last lens is needed to collimate the beam so that it is roughly the size of the photoreceiver. The neutral density (ND) filter in front of the photoreceiver is critical to attenuate

the damaging amount of power the setup is capable of delivering. The SHG needs to be tested through a wide range of powers, so for convenience two wheel mounts were used to allow for fast swapping out of neutral density filters; one for course one for fine.

On the green output side of the dichroic there is a camera used to view the output of the SHG cavity. This camera will show obvious cavity misalignments. There is also a photodiode used for power measurements and a beamsplitter to break the beam into two constituents for the two detectors.

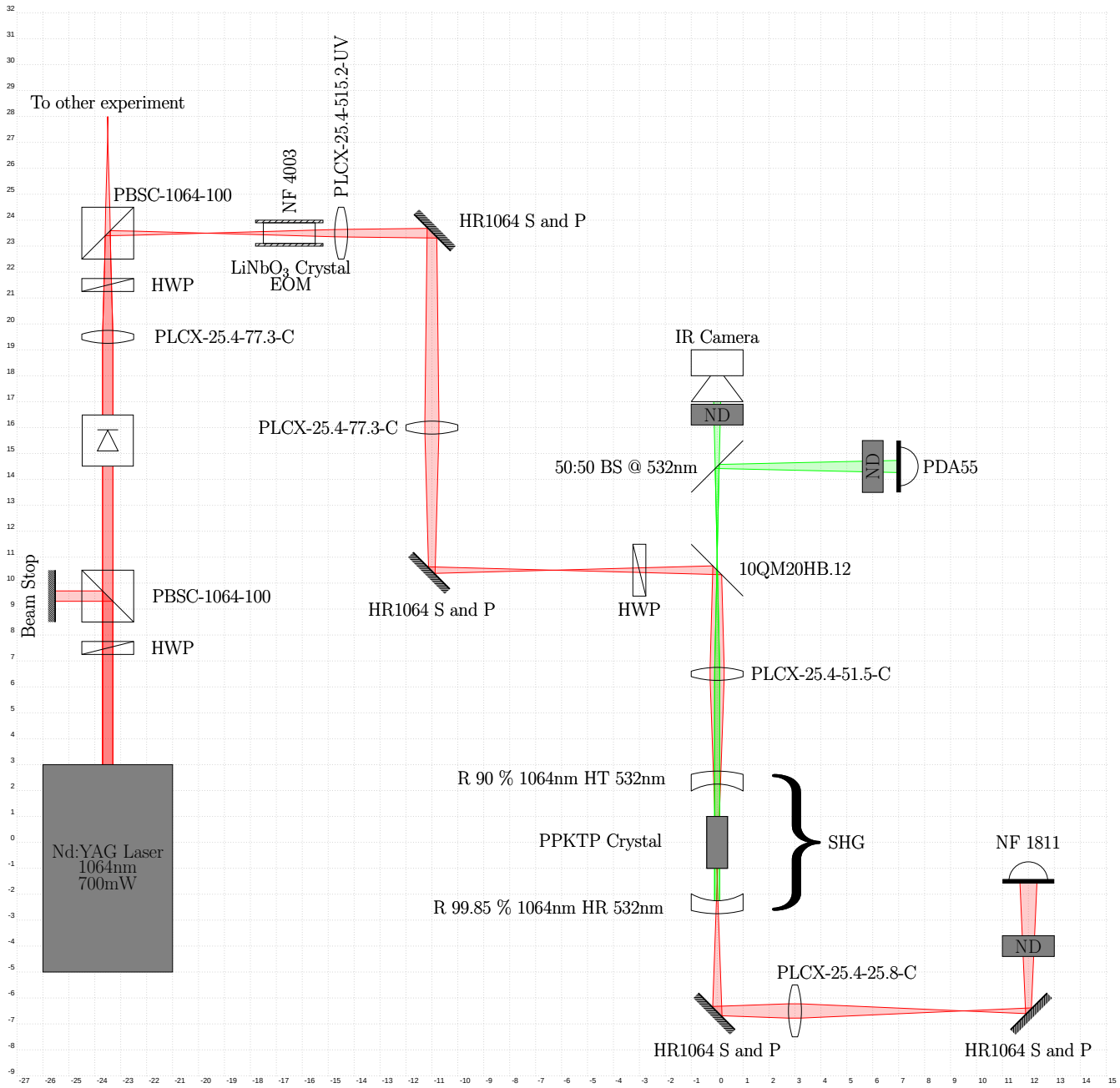

Figure 10: Optical Experimental Layout. Each division is equal to one inch. Positions of beam waists are relatively accurate. Components and beams are not to scale, but their positioning relative to the center of the SHG is. The components in the SHG have been enlarged and their positioning is not to scale.

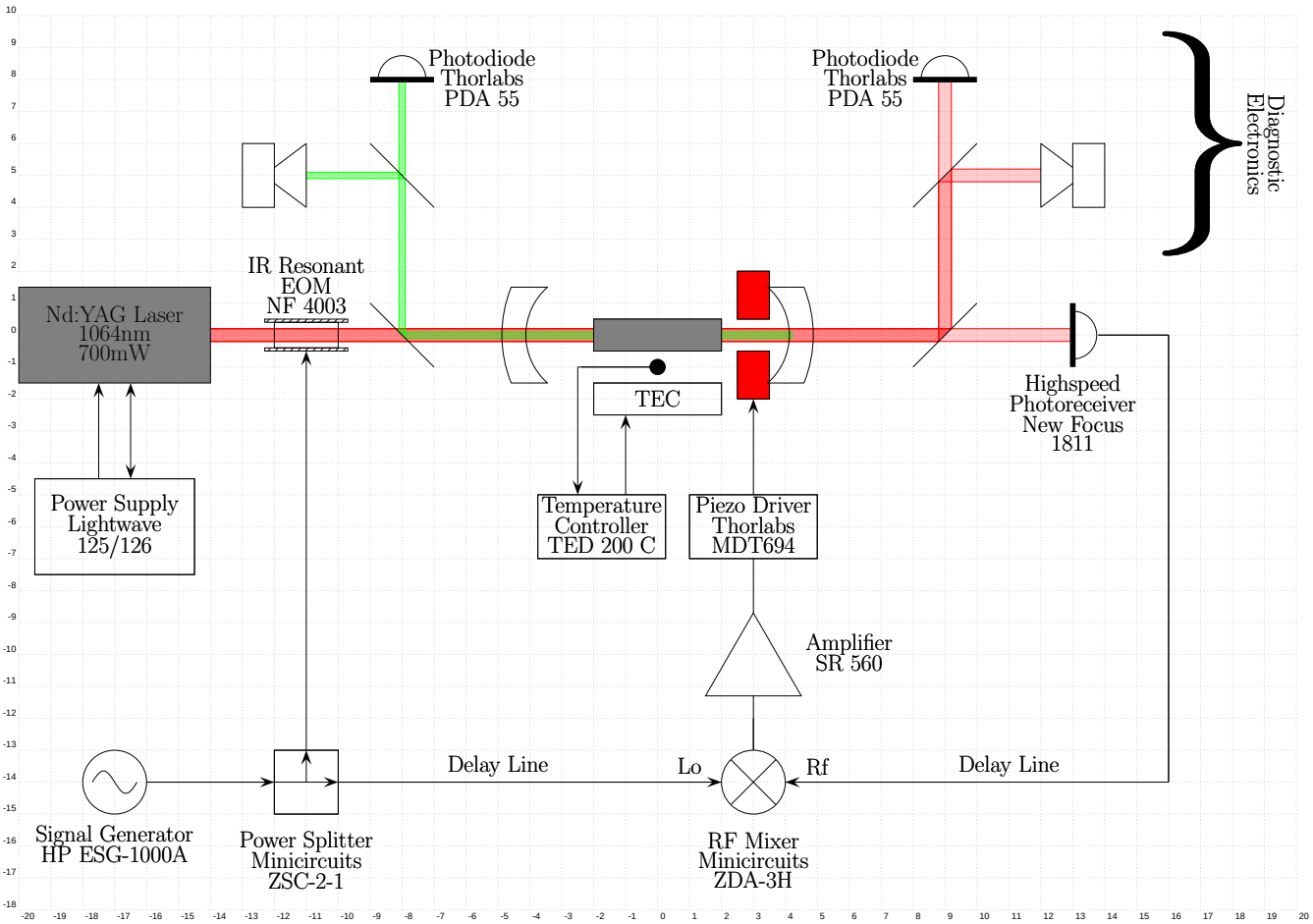

Figure 11: ?

8 Tuning

In practice Mode-Matching and Cavity Alignment may have to be iterated through several times.

8.1 Mode Matching

In this section one method of mode matching is put forth.

1. Determine the waist size and location of the beam coming from the laser. This is done by taking waist size measurements with a beam analyzer at two or more locations.

2. Fit the equation

$$w(z) = w_0\sqrt{1 + \left(\frac{\lambda(z - z_0)}{\pi w_0^2}\right)^2} \tag{47}$$

   [5, Eq. 20] to the data taken in the previous step to obtain a least square regression solution for z_0 and w_0.

3. Based on the geometry of the cavity calculate the proper input mode for the SHG. A symmetric cavity will have a waist located at the center, the size of which is given by

$$w_0 = \sqrt{\frac{\lambda}{2\pi}\sqrt{d(2R - d)}} \tag{48}$$

[5, Eq.48]. Our SHG has focusing lenses built into the mirrors which change the required input beam. The SHG will thus require a waist of size

$$w = \pm \frac{2 f w_0 \lambda}{\sqrt{4\pi^2 w_0^4 + (d_0 - 2f)^2 \lambda^2}} \tag{49}$$

located at

$$d = \frac{f[4\pi^2 w_0^4 + d_0(d_0 - 2f)\lambda^2]}{4\pi^2 w_0^4 + (d_0 - 2f)^2 \lambda^2} \tag{50}$$

where d is measured from the center of the cavity, d_0 is the length of the cavity, R is the radius of curvature of the mirrors, f is the focal length of the focusing mirrors that are built into the mirrors, and λ is the wavelength. Equations 49 and 50 were derived by converting the location and size of the waist inside the cavity to one outside the cavity by a focusing lens. (give the equations that were used to derive them?) For our cavity (give the values)

4. Now we know (experimentally) what the laser mode is, and we know (theoretically) what the input mode should be. We can perform mode matching calculations to determine a lens configuration that will convert one mode into another. A tutorial on mode matching is beyond the scope of this paper.

5. Once the calculation is complete and the array of optics in place the beam should be decently well mode-matched. Place the SHG in the position dictated by the calculation.

6. Try to adjust the cavity length to find a resonance. At this point that cavity and laser are probably sub-optimally coupled, but close enough that a significant amount of light can get through. Working with a symmetric cavity has the added advantage of permitting us to see what the cavity wants by observing what the cavity passes. Determine the waist size and location of the beam transmitted through the cavity in the same manner as before.

7. Perform another mode-matching calculation with the more accurate empirical data. The mode-matching optics shouldn't have to be moved far.

8. This process can be reiterate to get closer and closer the ideal.

8.2 Cavity Alignment

Here a proven method for aligning the mirrors of the cavity is furnished.

1. The first step in cavity alignment is prepping the beam. It needs to enter the SHG at the correct height. Additionally it should coincide perfectly with the axes of the cavity. This id done with the SHG removed from the optics table for the time being.

2. Place a beam alignment marker as close to the last mirror before the SHG as possible. Adjust the mirror before this (second to last mirror before SHG) so that the beam goes through the center of the beam alignment marker.

3. Remove this alignment marker, and place one as far away from the last mirror before the SHG as possible. This should be done without any optical elements being between the alignment marker and last mirror before the SHG.

4. Adjust the last mirror before the SHG to get the beam to go through the alignment marker.

5. Reinstate the first alignment marker. Move the second to last mirror so the beam goes through the first marker.

8.3 Optimizing PDH

Phase matching mixer inputs: -The transmitted rf is extremely weak. to maximize -bring the cavity close to resonance -cranck up the laser power so the transmitted power is high enough where we fee comfortable exposing the photoreceiver to it -cranck up the RF until it is close to the maximum allowable for the EOM -this is all we can do to maximize the RF hitting the photoreceiver -plug photoreceiver out and synth out into scope -adjust cable length so that the two waves are 90 deg out of phase -the photoreceiver signal may still be too small to register in which case a high gain, low noise amp could be used, but it's going to effect the phase.

Construct the above circuit. The round trip of the RF traveling from the power splitter, to the EOM, through the laser beam, from the photoreceiver and to the mixer should differ by half a wavelength from the round trip distance from the power splitter to the mixer. This is equivalent to matching the phase of the two signals going into the mixer. If they are 180 degrees out of phase this will invert the PDH error signal which is fine, the signal can be inverted on the amplifier. However, if the they are 90 degrees out of phase the error signal will vanish.

Ideally when there is no laser signal there is no PDH error signal

-ground sr560 input and zero dc offset for better results. -gain should be as high as possible without overloading. gain is $2 * 10^4$. -use the dc offset of the piezo driver to find a resonance. Then sweep the piezo driver offset up until the SR560 cannot compensate.

-DC coupling must be used on the amp!

-more light impinging on the rf photoreceiver yields a stronger error signal, however the photoreceiver is easily damaged so don't run it too close to the damage threshold.

-explain what gain does on the sr560 -explain what the lo-pass filter is for on the sr560 -why do we use 24.48MHz? -why use a piezo instead of changing the laser frequency?

-somewhere talk about how the input mode is a function of cavity length, but changes on the order of one wavelength have negligible effect. Show this with a taylor expansion?

-Graph of pdh error signal as a function of ppktp crystal temperature to show how temperature changes change the index of refraction which changes effective cavity length which pdh tries to compensate for, but if cavity length changes too much pdh error signal clips and cavity falls out of resonance.

8.4 The Cavity Scan Method of Mode Matching

This method relies on the fact that transverse modes have resonant frequencies specific to that mode. This technique will not work for perfectly (concentric??) cavities though, because this is the one case where all resonant frequencies are degenerate.

1. Some changes to the wiring for the PDH method have to be made. Hook a function generator's output up to channel 1 of the oscilloscope, disconnect the PDH error signal from the piezo driver and hook it up to ch. 2 on the oscilloscope (may have to switch impedances), and hook the piezo driver input up to function generator's output.

2. Place photodiodes (shown as diagnostic electronics in figure 11) to detect the second harmonic and transmitted fundamental. Hook them up to the scope.

3. Set the function generator to 5-10Hz. The cavity shouldn't be driven too fast because the piezo-mirror system has inertia and doesn't react instantly, also it takes time for the cavity to reach a steady state (realistically the free spectral range is so high that the time the cavity takes to build up to a steady state is negligible). The cavity should also be driven fast enough so that the experimenter can tell what effect any adjustment has on the cavity. Viewing the modes with a TV camera can be useful, but this means the cavity has to be driven slowly enough so the eye can discern the changes (24Hz absolute max).

4. amplitude is 1 or 2 Vpp. use triangle waveform. You do not want to drive the cavity through one free spectral range. Doing so will give the false impression of higher order modes.

5. Adjust the quiescent voltage of the piezo until a maximum (in transmitted / second harmonic light) is found where the the function generator signal crosses zero.

-the cavity scan method of mode matching is also a good way to set the piezo bias (quiescent) voltage. -this method will not work for a perfectly confocal cavity (as mentioned before, in a perfectly confocal cavity the resonance frequencies of each mode are exactly degenerate for a confocal cavity which means the cavity scan won't work) P.438 in siegman

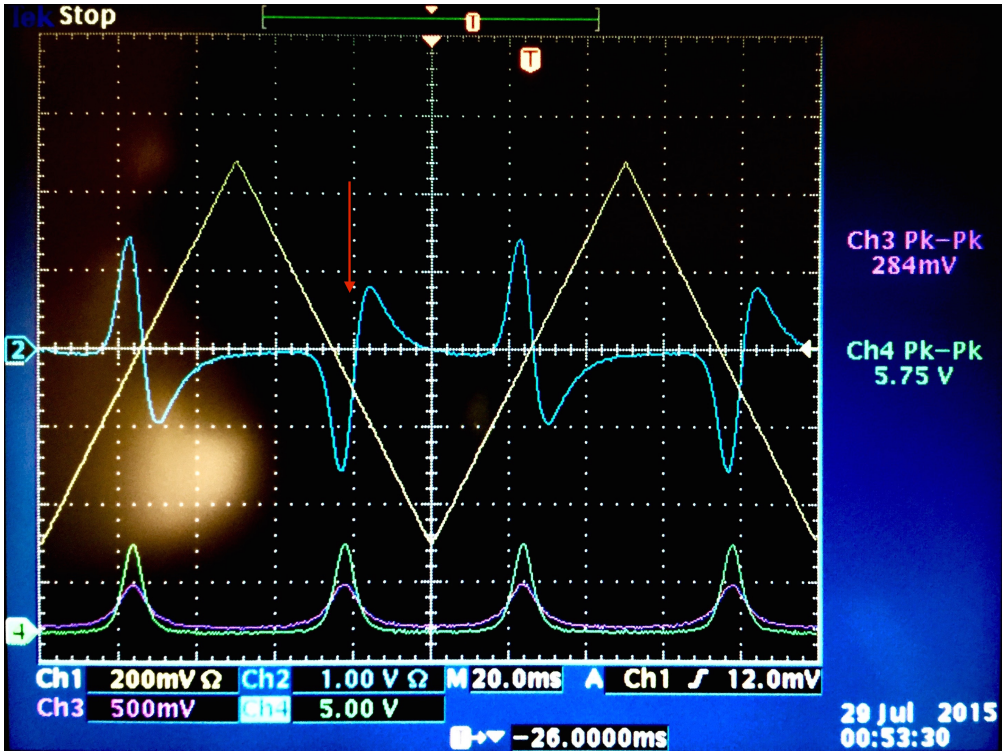

Figure 12: Yellow–Function generator out; Blue–PDH error signal; Green–Second harmonic power; Purple–Transmitted power. Light colored smudge on left of image is glare on the screen.

(Give a graph of what good and bad modematching will look like)

8.5 The Ideal Cavity Type (Is this the best place for this section?)

9 Modifications to the SHG

10 Results

-conversion efficiency -as a function of temperature -as a function of laser power

To calculate the efficiency of the SHG we use photodiodes to measure beam power in several places. The formula

$$P = \frac{1}{r(\lambda)ga}V \tag{51}$$

gives the conversion factor from volts out to power in, where $r(\lambda)$ is the responsivity (which is a function of wavelength), g is the transimpedance gain, and a is the attenuation coefficient.

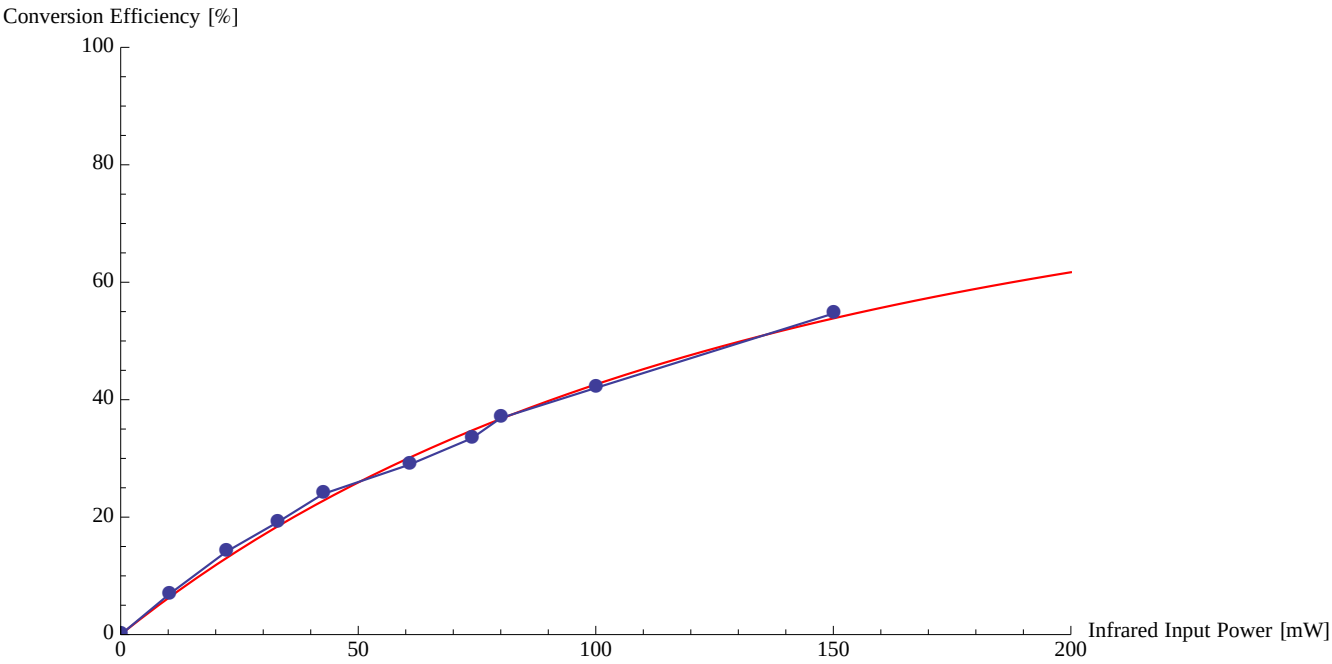

Figure 13: ?

11 Appendix A: Supplemental Mathematics to Theory Section

The second-order term in equation 8 contains the tensor product

$$\mathbf{E}^{\otimes 2} = \begin{pmatrix} E_x^2 & E_x E_y & E_x E_z \\ E_y E_x & E_y^2 & E_y E_z \\ E_z E_x & E_z E_y & E_z^2 \end{pmatrix} \tag{52}$$

There are 9 elements in this matrix, but note the components of the electric field commute $E_i E_j = E_j E_i$, so there are really only 6 unique terms. Additionally (for reasons beyond the scope of this paper?) the second-order susceptibility tensor $\chi^{(\mathbf{2})}_{\mathbf{ijk}}$ is symmetric under a permutation of its last two indices

$$\chi^{(\mathbf{2})}_{\mathbf{ijk}} = \chi^{(\mathbf{2})}_{\mathbf{ikj}} \tag{53}$$

Which invites us to use the Voigt abbreviated notation (which is a to reduce the order of a symmetric tensor) to define an *effective SHG coefficient*

$$\mathbf{d_{il}} = \frac{1}{2}\chi^{(\mathbf{2})}_{\mathbf{ijk}} \tag{54}$$

The relation between the subscripts l and jk are given by the table below.

l	1	2	3	4	5	6
jk	xx	yy	zz	zy	zx	xy
				yz	xz	yx

Table 3: Voigt abbreviated notation. [**?**]

Which brings us to the conventional way of writing the second-order term in equation 8

$$\mathbf{P^{(2)}} = \epsilon_0 \begin{pmatrix} d_{11} & \dots & d_{16} \\ d_{21} & \dots & d_{26} \\ d_{31} & \dots & d_{36} \end{pmatrix} \begin{pmatrix} E_x^2 \\ E_y^2 \\ E_z^2 \\ 2E_yE_z \\ 2E_zE_x \\ 2E_xE_y \end{pmatrix} \tag{55}$$

[**?**]

Now what happens if we pass a laser beam through a non-linear medium? For a monochromatic and coherent beam we can write the electric field as

$$\mathbf{E}(\mathbf{r},t) = \Re\left\{\mathbf{E_0}e^{i(\mathbf{k}\cdot\mathbf{r}-\omega t)}\right\} \tag{56}$$

If we plug this into eq (above) and assume only first and second order effects are appreciable we have

$$\mathbf{P}(\mathbf{r},t) = \mathbf{P_0^{(1)}}\Re\left\{e^{i(k\cdot r-\omega t}\right\} + \mathbf{P_0^{(2)}}\Re\left\{1+e^{2i(k\cdot r-\omega t}\right\} \tag{57}$$

$$E_iE_j = \frac{1}{2}\Re\left\{E_{0i}E_{0j}\left(1+e^{-2i\omega t}\right)\right\} \tag{58}$$

$$\begin{aligned} \mathbf{P^{(2)}} &= \frac{\epsilon_0}{2}\Re\left\{\begin{pmatrix} d_{11} & \dots & d_{16} \\ d_{21} & \dots & d_{26} \\ d_{31} & \dots & d_{36} \end{pmatrix} \begin{pmatrix} E_x^2 \\ E_y^2 \\ E_z^2 \\ 2E_yE_z \\ 2E_zE_x \\ 2E_xE_y \end{pmatrix}\left(1+e^{-2i\omega t}\right)\right\} \qquad (59) \\ &= \Re\left\{\mathbf{P_0^{(2)}}\left(1+e^{-2i\omega t}\right)\right\} \qquad (60) \end{aligned}$$

12 Appendix B

Let the electric field of an incoming photon be given by

$$\mathbf{E} = \frac{1}{2}\left(\mathbf{E_0}e^{i(\mathbf{k}\cdot\mathbf{r}-\omega_0 t)} + \mathbf{E_0}^* e^{-i(\mathbf{k}\cdot\mathbf{r}-\omega_0 t)}\right) \tag{61}$$

Examining equation (2) we see $\mathbf{E}$ is not exactly "squared", but instead contains every possible product of two components of $\mathbf{E}$ so we calculate

$$E_iE_j = \frac{1}{2}\Re\left\{E_{0i}E_{0j}\left(1+e^{i(2\mathbf{k}\cdot\mathbf{r}-2\omega_0 t)}\right)\right\} \tag{62}$$

Plugging this result into equation (2) we find

$$\mathbf{P^{(2)}} = \epsilon_0 \begin{pmatrix} d_{11} & \dots & d_{16} \\ d_{21} & \dots & d_{26} \\ d_{31} & \dots & d_{36} \end{pmatrix} \begin{pmatrix} E_x^2 \\ E_y^2 \\ E_z^2 \\ 2E_yE_z \\ 2E_zE_x \\ 2E_xE_y \end{pmatrix} \tag{63}$$

13 Appendix C: Gaussian Beams (and higher order eigenmodes of the paraxial wave equation in free space?)

Waves in homogenous and isotropic space satisfy the wave equation [9, Eq. 16.1]

$$\left[\nabla^2 + k^2\right] \vec{E} = \vec{0} \tag{64}$$

The simplest non-trivial solutions to which are infinite plane and spherical waves:

$$\begin{array}{rl} \text{Infinite Plane Wave} & \vec{E_0} \exp[-i(\vec{k} \cdot \vec{r} + \omega t)] \\ \text{Spherical Wave} & \vec{E_0} \exp[-i(kr + \omega t)] \end{array}$$

These two solutions are not realistic, however, because they carry infinite power through any surface enclosing the source.

(some transition needed)

To find the shape of the wave envelope, call it u, factor out

$$\vec{E}(\vec{r}) = \vec{u}(\vec{r}) e^{-i\vec{k}\cdot\vec{r}} \tag{65}$$

(should that be a dot product in the exponent?)

(some transition needed)

For simplicity we will use the convention of taking $\hat{z}$ as the direction wave propagation.

The Paraxial Approximation assumes variation of the envelope in the z direction is much smaller than variation of u in the transverse plane (due to the finite size of the beam) and the oscillations of the field on the order of lambda due to the exp term which was factored out. Mathematically

$$\left|\frac{\partial^2 \mathbf{u}}{\partial z^2}\right| \ll \left|2k\frac{\partial \mathbf{u}}{\partial z}\right| \vee \left|\frac{\partial^2 \mathbf{u}}{\partial x^2}\right| \vee \left|\frac{\partial^2 \mathbf{u}}{\partial y^2}\right| \tag{66}$$

which means we can drop the $\partial^2\mathbf{u}/\partial z^2$ term in the exact wave equation (eq. num) which gives us the paraxial wave equation

$$\left[\nabla_{xy}^2 - 2ik\partial_z\right] \vec{u} = \vec{0} \tag{67}$$

the paraxial wave equation is valid for paraxial optical beams diverging or converging at cone angles up to roughly 30 deg; at angles smaller than 30 deg the d2u/dz2 term dropped from the wave equation to arrive at the paraxial wave equation is at least one order of magnitude smaller than any of the other terms. [9, P. 630]. Beams diverging at angles greater than 30 deg are very poorly culimated. Such beams are not encountered in this experiment so the paraxial wave equation is appropriate.

P.634 "Huygens' integral and the paraxial wave equation represent exactly the same mathematical (and physical) approximation."

Now we make the Fresnel Approximation. Taylor expand the r in the spherical wave equation (eq. num)

$$r = z + \frac{s^2}{2z} + \ldots \tag{68}$$

now plug this into the spherical wave equation and get

$$\vec{u}(\vec{r}) = \frac{\vec{u}_0}{z} \exp\left[-i\frac{ks^2}{2z}\right] \tag{69}$$

This is an exact solution to the paraxial wave equation. This also carries off infinite power through any enclosing surface. This is because the wave amplitude does not fall off with transverse distance from the optic axis.[p.638] (Validity of the Fresnel Approx P.634)

P.638 " This quadratic phase variation of course represents only a paraxial or Fresnel approximation to the true surface of a sphere, so that this form will have a sizable phase error if we move far enough out from the optic axis."

As of now all the wave solutions discussed have carried off infinite power. To resolve this generalize the radius of curvature in eq num , allowing it to be complex. The complex term is called the beam parameter, which brings us to the gaussian beam

——— relevant equations for gaussian beams — — —

This is just one solution to the paraxial wave equation. Because the differential operator in this equation is hermitical (IS THIS TRUE?) the solution set should be an infinite set of orthogonal basis functions. We will get to two complete sets in the following sections.

These are the solutions in free space.

13.1 Derivation of Hermite-Gaussian Modes

13.2 Derivation of Laguerre-Gaussian Modes

14 Appendix D: List of Electronics

Element	Manufacturer	Product
RF Attenuator	Mini Circuits	-10dB
Laser	Lightwave	NPRO M126N-1064-700
Laser Power Supply	Lightwave	125/126
IR Resonant Phase Modulator (EOM)	New Focus	4003
Photodiode	Thorlabs	PDA55
TEC Controller	Thorlabs	TED 200 C
Power Splitter	Minicircuits	ZSC-2-1
Signal Generator	HP	ESG-1000A
Preamp	Stanford Research	SR560
Photoreceiver	New Focus	1811
Piezo Driver	Thorlabs	MDT694
RF Mixer	Minicircuits	ZDA-3H
IR Camera	Thorelabs	
Television		
Oscilloscope	Tektronix	TDS 3034

Table 4: Summery of electronics used in this experiment.

15 Appendix E: List of Optics

Lens	Manufacturer	Focal Length @ 1064nm	Focal Length @ 530nm
PLCX-25.4-515.1-UV	CVI	1.0000 m	1.0000 m
PLCX-25.4-77.3-C	CVI	152.6 mm	148.8 mm
PLCX-25.4-51.5-C	CVI	101.7 mm	99.1 mm
PLCX-25.4-25.8-C	CVI	50.9 mm	49.7 mm

Table 5: Summery of lenses used.

Mirror	Manufacturer	R @ 1064nm	R @ 530nm
NF-5104			

Table 6: Summery of lenses used.

Beamsplitter / Dichroic	Manufacturer	Reflect	Transmit
10QM20HB.12	Newport	> 99.5% @ 1064nm	> 95% @ 532nm
BS1-1064-50-1025-45s	CVI	50% s-pol @ 1064nm	50% s-pol @ 1064nm
PBSC-1064-100	CVI	s-pol	p-pol

Table 7: Summery of lenses used.

Acknowledgments

Thank you Keith Riles for using your grant to fund this research. Richard Gustafson Jake Calcutt

References

[1] LIGO Scientific Collaboration Authors. Enhanced sensitivity of the ligo gravitational wave detector by using squeesed states of light. *Nature Photonics*, 117:613–619, July 2013.

[2] Eric D. Black. An introduction to pound-drever-hall laser frequency stabilization. *American Journal of Physics*, 69(1):79–87, January 2001.

[3] Carlton M. Caves. Quantum-mechanical noise in an interferometer. *Physical Review*, 23(8):1693–1708, April 1981.

[4] Mark Fox. *Quantum Optics: An Introduction*. Oxford University Press, UK, June 2006.

[5] H. Kogelnik, T. Li. Laser beams and resonators. *Proceedings of the IEEE*, 54(10):1312–1329, October 1966.

[6] K.R. Parameswaran, J.R. Kurz, R.V. Roussev, M.M. Fejer. Observation of 99generation in a periodically poled lithium niobate waveguide. *Optics Letters*, 27(1):43–45, January 2002.

[7] M.M. Fejer, G.A. Magel, D.H. Jundt, R.L. Byer. Quasi-phase-matched second harmonic generation: Tuning and tolerances. *IEEE Journal of Quantum Electronics*, 28(11):2631–2654, November 1992.

[8] R.W. Munn, C.N. Ironside, editor. *Principles and Applications of Nonlinear Optical Materials*. Chapman and Hall, first edition, 1993.

[9] Anthony E. Siegman. *Lasers*. University Science Books, 1986.